

NUMERICAL PREDICTION OF GROUND-BORNE NOISE AND VIBRATIONS IN BUILDINGS INDUCED BY PILE DRIVING

A. Colaço¹, P. Alves Costa¹, C. Mont'Alverne Parente¹ and A. Silva Cardoso¹

¹Construct-FEUP, University of Porto, Porto, Portugal
{aires@fe.up.pt, pacosta@fe.up.pt, cparente@fe.up.pt, ascardoso@reit.up.pt}

Resumo

O recurso a fundações indiretas por cravação de estacas é um dos métodos mais utilizados na indústria da construção aquando da presença de camadas superficiais com baixa capacidade de carga. A aplicação deste método construtivo em ambientes urbanos requer um conhecimento técnico e científico alargado acerca dos fenómenos de geração e propagação de vibrações, com ênfase para a sua interferência em edifícios próximos e o consequente incômodo dos ocupantes. Neste contexto, é apresentado um modelo numérico de previsão de vibrações e ruído re-radiado em edifícios induzidos pela cravação das estacas. O modelo é baseado numa abordagem subestruturada, englobando todo o meio de propagação, desde a fonte de vibração ao recetor. Como sistematização da ferramenta numérica, é apresentado um exemplo de aplicação onde são avaliados os níveis de vibração e ruído re-radiado no interior de um edifício, mostrando claramente a pertinência deste trabalho.

Palavras-chave: cravação de estacas, ambiente urbano sustentável, vibrações e ruído re-radiado, modelação numérica.

Abstract

Pile driving is an effective constructive method for foundations in shallow soil layers with low bearing capacity. Its installation generates the propagation of vibration through the ground that can damage structures or disturb people in the vicinity of the pile driving, requiring a significant level of knowledge from the scientific and technical communities about this phenomenon. In this context, this paper presents the mathematical formulation of a numerical approach for prediction of vibration and re-radiated noise induced by pile driving based in a sub-structuring methodology, where the whole propagation media is considered, from the vibration source to the receiver. A case study is presented, where the vibrations and re-radiated noise levels inside the building are assessed, clearly showing the pertinence of this work.

Keywords: pile driving, sustainable urban environment, ground-borne noise and vibrations, numerical modelling.

PACS no. 43.40.At, 43.40.Kd

1 Introdução

When dealing with shallow soil layers with low bearing capacity, pile driving presents some advantages, namely in what concerns to construction time, automation and industrialization of construction procedures among others, being one of the most aged methods for foundations construction. However, some environmental drawbacks are associated, especially in what concerns to the generation of ground-

borne vibrations that propagate over the soil layers and interact with existing buildings, causing damage of equipments and structures or disruption to people and activities located in the vicinity [1, 2]. The difficulty of predicting these vibrations in many cases prevents the use of this pile installing method, with considerable losses from technical and economic points of view. In order to avoid these occasional structural damages or the disturbance of the surrounding buildings occupants, it is of the utmost importance that the level of vibrations, as well as the re-radiated noise, could be estimated prior to the beginning of pile driving.

Despite the vast majority of the studies performed about ground vibrations induced by pile driving being based on empirical models [3, 4], the numerical modeling can be considered as an alternative approach, probably complementary, allowing to generalize the applicability of the empirical laws in different scenarios and locations. One of the first attempts to deal with the problem was made by Ramshaw et al. [5] using a finite-infinite element model to simulate the pile-ground system in axisymmetric conditions. The same procedure was followed by Khoubani et al. [6]. Homayoun Rooz [7] uses the finite elements commercial software Abaqus, imposing artificial boundaries based on a gradual increase in the soil damping to prevent wave reflection. Masoumi et al. [8, 9] gave a relevant contribution in this field, proposing a coupled FE-BE model based on a subdomain formulation. The authors, in Parente et al. [10], presented a preliminary study on the topic, where an axisymmetric FEM-PML model was proposed. The combination between Finite Elements and Perfect Matched Layers gives rise to a very efficient method for dealing with this problem, being the treatment of the artificial boundaries by PML one of the most promising methods to avoid spurious reflections alongside the truncation boundaries.

The above cited works have in common the fact of being only focused in the prediction of the response at the ground surface. In fact, there is a lack of studies concerning to the prediction of the building response in terms of vibrations and re-radiated noise due to pile driving. Vibrations and re-radiated noise are two deeply connected phenomena, and a common approach in the study of the pernicious effects induced inside the buildings is recommended [11]. One efficient way for the modelling of whole system is following a substructuring approach that selects the most appropriate numerical techniques to deal with the specificities of each subdomain and then couples them according to the required compatibility and equilibrium conditions [12, 13]. Thus, an additional sub-model is required, i.e., a model for the simulation of the dynamic response of the building (receiver) due to the excitation induced by vibrations generated by pile driving. In this sense, a common methodology is the consideration of the soil-structure interaction (SSI) problem through a combination between a 3D finite element model (FEM) for the structure and a lumped-parameter model [14, 15] or a Boundary Element Model (BEM) [16, 17] for the ground.

In terms of re-radiated noise prediction, different prediction models have been proposed, with different complexity levels and applications [18-21]. The authors, in Colaço et al. [22], have also worked in this topic, proposing a 3D FEM-MFS hybrid numerical model for vibro-acoustic prediction, where the Finite Element Method (FEM) is used to evaluate the structural response and the Method of Fundamental Solutions (MFS) is adopted to assess the acoustic response inside a closed space.

Thus, the objective of this paper is to present an efficient numerical approach for the prediction of vibrations and re-radiated noise induced in buildings due to pile driving operations in the vicinity. The model comprises the simulation of the whole system, from the excitation source to the building response in terms of vibrations and re-radiated noise. After the model presentation, a simple case study is developed where the main physical features of the dynamic phenomena induced by pile driving are investigated.

2 Numerical model

2.1 Generalities

The numerical model propose is based in a sub-structuring approach, being split into four main modules: one comprises the pile-ground model, modelled by an axisymmetric FEM-PML approach; the second one regards to the dynamic simulation of the hammer device; the third one is related with the modelling of the building through a 3D FEM approach and taking into account the soil-structure interaction (SSI); the last one comprises the acoustic domain, adopting a 3D MFS approach. The final goal is the assessment of groundborne noise and vibration levels inside buildings due to pile driving in the vicinity. Figure 1 shows the interaction scheme and the main aspects and assumptions of the methodology are described following.

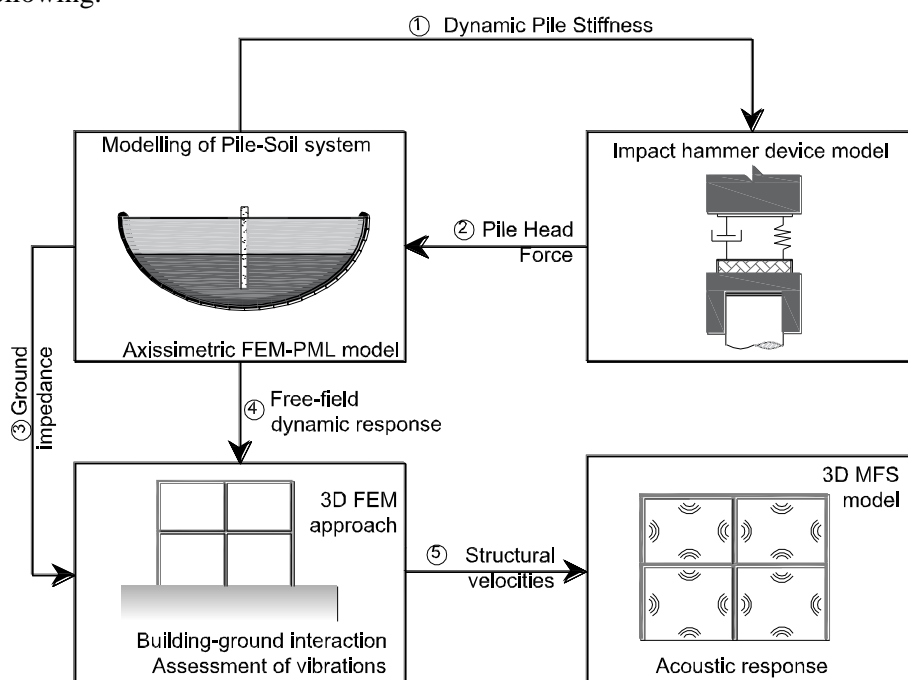


Figure 1 – Scheme of the numerical modelling approach proposed.

2.2 Modelling of pile-ground system

The pile-ground dynamic response induced by pile driving is computed by a numerical procedure based on the coupling between the finite elements and perfectly matched layers (PML's) methods. The PML layer is adopted to treat the boundary effects inherent to the truncation of the domain associated to the finite element discretization, avoiding the spurious reflection of waves. This methodology is formulated in the frequency domain and the three-dimensional (3D) response of the system is obtained through an axisymmetric formulation.

Following this approach and after the assemblage of the equations of each individual element, the equilibrium condition in the frequency domain is established by the following equation:

$$\{([K] + [K^*(\omega)]) - \omega^2([M] + [M^*(\omega)])\}u(\omega) = \{p(\omega)\} \quad (1)$$

where ω is the frequency, u is the vector of nodal displacements and p is the vector of external nodal loads. The matrices $[K]$ and $[M]$ are the global stiffness and mass matrices of the FEM. According to the classic finite elements notation, it comes out that:

$$[K] = 2\pi \int_S B^T D B r dS \quad (2)$$

$$[M] = 2\pi \int_S N^T \rho N r dS \quad (3)$$

where ρ is the volumetric mass, $[B]$ is the strain matrix, $[D]$ is the strain-stress matrix and $[N]$ is the shape function matrix.

$[K^*]$ and $[M^*]$ are the corresponding global stiffness and mass matrices for the PML domain:

$$[K^*(\omega)] = 2\pi \int_y \int_x B^{*T} D B^* r \lambda_x \lambda_y dx dy \quad (4)$$

$$[M^*(\omega)] = 2\pi \int_y \int_x N^T \rho N r \lambda_x \lambda_y dx dy \quad (5)$$

being $[B^*]$ the strain matrix in the stretched domain and λ_x and λ_y are the stretching functions in the x and y directions, respectively. Additional information about this procedure can be found in Parente et al. [10].

2.3 Hammer model and hammer-pile interaction

In the context of the prediction of vibration induced by pile driving, the time history of the force generated by the hammer impact is required. For that, the impact hammer system can be simulated as a two degrees of freedom model as depicted in Figure 2, representing a free-falling weight (ram) that impacts the anvil at the pile head, represented as a hammer cushion and a pile cap or helmet. These two masses are separated by a spring which reproduces the cushion stiffness. In fact, the cushion deforms itself in a non-linear way and yet absorbs energy. With the aim of representing this non-linearity and the energy loss, it is possible to model the cushion as a linear spring in parallel with a dashpot [23].

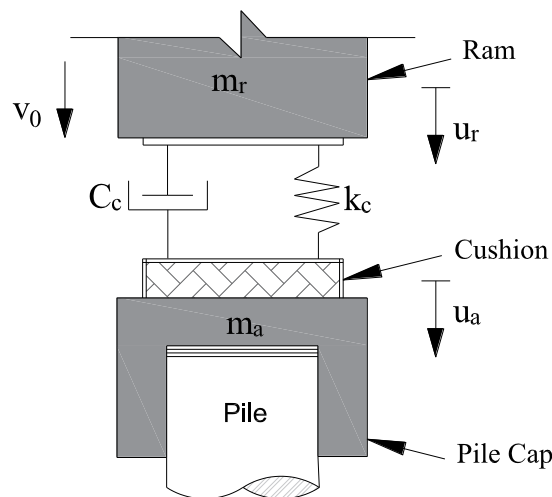


Figure 2 – Two degrees of freedom pile-hammer model.

The dynamic damped model can be translated by the system of equations expressed in eq. (6), considering a pseudo-force application whose value is equal to the modulus of the momentum transferred from the ram to the pile.

$$(-w^2 \begin{bmatrix} m_r & 0 \\ 0 & m_a \end{bmatrix} + iw \begin{bmatrix} c_c & -c_c \\ -c_c & c_c \end{bmatrix} + \begin{bmatrix} k_c & -k_c \\ -k_c & k_c + k_p \end{bmatrix}) \times \begin{bmatrix} u_r \\ u_a \end{bmatrix} = \begin{bmatrix} m_r v_0 \\ 0 \end{bmatrix} \quad (6)$$

where m_r is the ram mass; m_a is the anvil mass, k_c and c_c are the stiffness and damping coefficient of the cushion, v_0 is the impact velocity of the ram and k_p is the pile dynamic stiffness. In relation to the last component, the pile dynamic stiffness can be analogous to the ratio between the force applied at a point in the pile head, $P(w)$, and its vertical displacement, $u_z(w)$. can be calculated from:

$$k_p(w) = \frac{P(w)}{u_z(w)} = \frac{1}{u_z(w)} \quad (7)$$

The pile head force in the frequency domain is obtained by means of the product between the pile dynamic stiffness, k_p , and the anvil displacement, u_a .

Since the anvil surface force is achieved by assuming a linear elastic model, tractions are generated at the moment of the ram rebound. This effect is due to a weakness of the models, which cannot represent the loss of contact between bodies owing to its elastic nature. However, Parente et al. [10] proposed a two steps computation approach to overturn this non-linear aspect.

In order to achieve the response in terms of nodal displacements, the multiplication between the respective transfer functions and the pile head force spectrum in the frequency domain should be performed. Posteriorly, time domain response is obtained by an inverse Fourier transformation of the signal.

2.4 Modelling of the building and soil-structure interaction

In terms of the modelling of the structure and its interaction with the remaining system, the procedure presented by Lopes et al. [7, 8] is followed. Thus, and briefly, eq. (15) represents the general equation of motion of the system, in the frequency domain, adequately adapted to take into account the soil-structure interaction:

$$\begin{bmatrix} K^{aa} & K^{ab} \\ K^{ba} & K^{bb} + K_s \end{bmatrix} \begin{bmatrix} u_a \\ \Delta u^b \end{bmatrix} = - \begin{bmatrix} K^{aa} & K^{ab} \\ K^{ba} & K^{bb} \end{bmatrix} \begin{bmatrix} 0 \\ u_0 \end{bmatrix} \quad (8)$$

where the term K^{ii} corresponds to the dynamic stiffness matrix of the structure, obtained by a 3D FEM model; u_0 is the incident wavefield (in terms of displacements), obtained from the response computed by the model presented in previous section; and the term K_s corresponds to the impedance of the soil, computed, in this specific case, by the lumped-parameter model expressed in Figure 3.

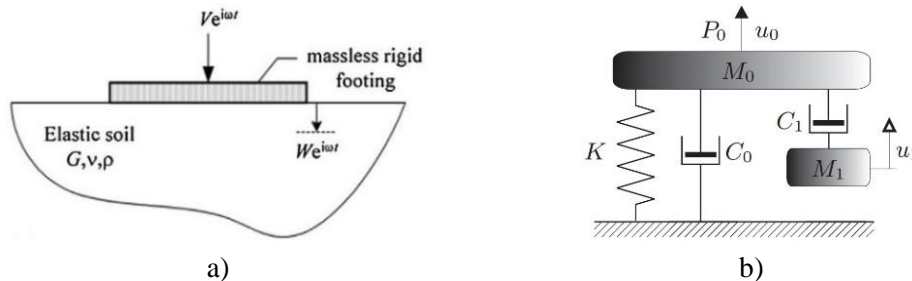


Figure 3 – Monkey-tail model: (a) problem description and (b) structural system [19].

2.5 Acoustic domain

The computed structural vibration velocities are imposed as boundary conditions for the assessment of the sound pressure levels generated within the building. The Method of Fundamental Solutions (MFS), previously experimental validated in Colaço et al. [22], is used for this task. In a brief way, this is a collocation method that allows describing the response of the acoustic medium through a linear combination of fundamental solutions (Green's functions) of the governing differential equation – the Helmholtz equation – obtained from a set of virtual sources positioned outside the propagating domain, as represent in Figure 4.

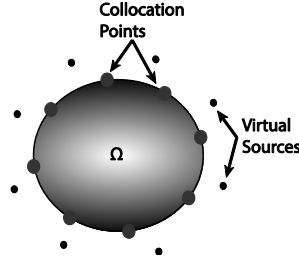


Figure 4 – Schematic representation of an MFS model for the acoustic domain Ω .

The acoustic response at a generic interior point x is then reproduced by considering the effects of NS virtual sources located outside the interest domain, as expressed by the summation in equation (9).

$$p(x, k_a) = \sum_{m=1}^{NS} A_m G^{3D}(x, x_0^{(m)}, k_a) \quad (9)$$

In this equation, $G^{3D}(x, x_0^{(m)}, k_a)$ corresponds to the Green's function of the sound pressure, which can be written as:

$$G^{3D}(x, x_0^{(m)}, k_a) = \frac{e^{-ik_a r}}{r} \quad (10)$$

where $x_0^{(m)}$ represents the coordinates of the virtual source m (with $m=1,2,\dots,NS$); r corresponds to the distance between the source and the receiver where the pressure is being evaluated. To complete this process, it is necessary to prescribe boundary conditions at the collocation points, resulting in a linear system of equations that determines the unknown amplitudes of the virtual sources, A_m . Thus, in the case of prescription of normal velocities at the boundary, the unknown amplitudes, A_m , can be obtained by the following relation:

$$\sum_{m=1}^{NS} [A_m H^{3D}(x_p^{(i)}, x_0^{(m)}, k_a, \vec{n})] = v_{n,i} \quad (11)$$

where $H^{3D}(x_p^{(i)}, x_0^{(m)}, k_a, \vec{n})$ corresponds to the Green's function for particle velocities. In this expression, the Green's function for particle velocities, $H^{3D}(x_p^{(i)}, x_0^{(m)}, k_a, \vec{n})$, is:

$$H^{3D}(x_p^{(i)}, x_0^{(m)}, k_a, \vec{n}) = \frac{1}{-i\rho\omega} \frac{(-ik_a r - 1)e^{-ik_a r}}{r^2} \frac{\partial r}{\partial \vec{n}} \quad (12)$$

where $x_p^{(i)}$ corresponds to the coordinates of the collocation point i (with $i=1,2,\dots,NP$); \vec{n} represents the orthogonal direction to the boundary; and ρ and c are the medium density and sound propagation velocity, respectively.

3 Application example

3.1 General description

The present study aims to identify the main behaviour trends of the pile-ground-building system, in terms of vibrations and re-radiated noise, due to pile driving. Figure 5 gives a general overview of the configuration adopted for the numerical example.

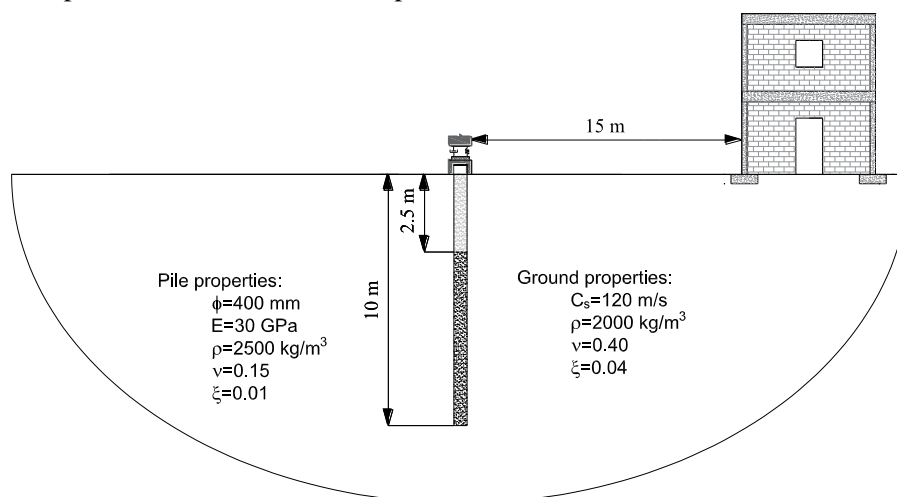


Figure 5 – Case study geometry.

For the sake of simplicity, it was assumed that the medium can be handled as a homogeneous halfspace. Two driving depths scenarios have been simulated, considering an impact applied on pile with a diameter of 400 mm, at penetration depths of 2.5 m and 10 m. The elastodynamic properties for pile-ground system are depicted in Figure 5.

Regarding the driving device, masses related to the ram and the anvil are equal to $m_r = 6860$ kg and $m_a = 850$ kg, respectively. For the hammer cushion, stiffness and damping values of 1.6×10^6 kN/m and 588 kNs/m, respectively, are considered. It is also assumed that the hammer hits the anvil with an initial velocity of 3 m/s.

In what concerns to the receiver, a two-story conventional building, with a total height of 6 m and a plan area of 5×5 m² is considered. This building has a structural scheme composed by a set of reinforced concrete elements: columns, beams and slabs, with sections of 20×20 cm², 20×40 cm² and 20 cm thickness, respectively. The building is contour by masonry infill walls, with thickness of 15 cm, Young modulus of 1.2 GPa, mass density of 1200 kg/m³ and Poisson's ratio of 0.2 [24]. The structure is supported by 4 concrete square spread footings, with 1.0 m of edge and a height of 0.35 m. The minimum distance between the pile and the building is 15 m.

3.2 Free-field dynamic response

The ground medium is discretized in a FEM mesh with 31700 triangular elements with 6 nodes. Taking advantage of the axisymmetric formulation conditions, the problem is solved as a two-dimensional problem and the pile centreline axis corresponds to the axisymmetric axis. The PML layers are coupled along the remaining system.

The analyses have been carried out for two possible embedment depths of the pile, such as 2.5 m and 10 m. General analysis of the results allows concluding the load transmitted to the pile head is dependent on the pile embedment depth. Time domain records show that larger force is related with the increase

of pile depth. On the other hand, the analysis on the frequency domain shows that considerable differences are observed in the frequency content of the load. For the embedment depth of 2.5 m, not only the peak value of the load is smaller, but there is also a concentration of the energy in frequency range up to 60 Hz. When the pile embedment achieves 10m, the frequency content is broader, with the larger percentage of energy concentrated for the frequency range up to 120 Hz. These differences on the hammer-pile interaction load are justified by the change of the pile-ground dynamic stiffness, since remaining variables are kept constant in both analyses. Actually, the larger the pile embedment depth, greater is the dynamic pile-ground stiffness, which justifies the increase of the dynamic interaction load.

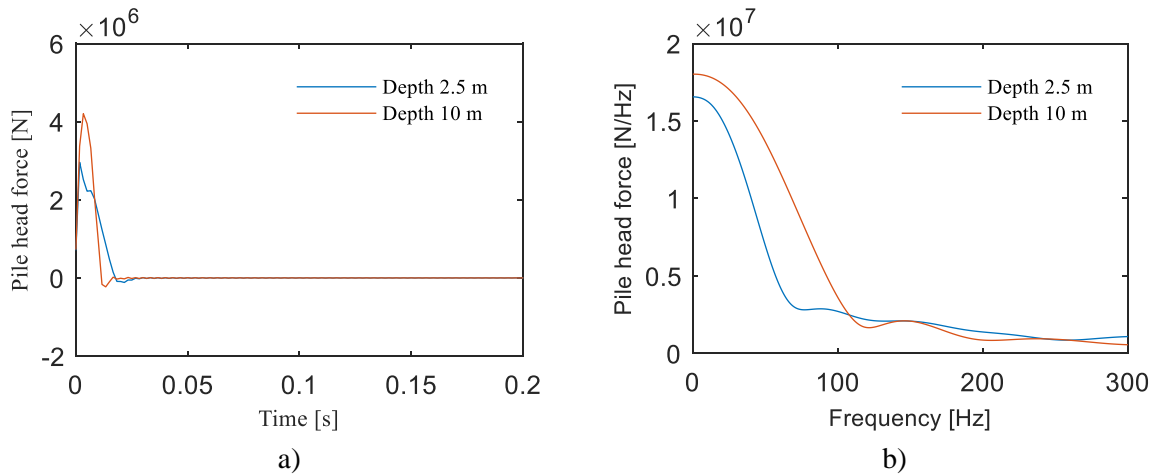


Figure 6 – Pile Head Force for penetration depths of 2.5 m (blue line) and 10 m (red line) in the a) time domain; b) frequency domain.

Figure 7 shows the time history of particle velocity for an observation point located at the ground surface and 15 m away from the pile center, coincident to the closest building foundation. The peak vibration values are larger for the shallow embedment pile depth although the fact of the lower value of the load applied on the pile head (see Figure 6). It is also possible to see that dominant frequency is in a lower range when pile embedment depth is equal to 2.5 m, comparatively to a scenario where the pile embedment depth is equal to 10 m.

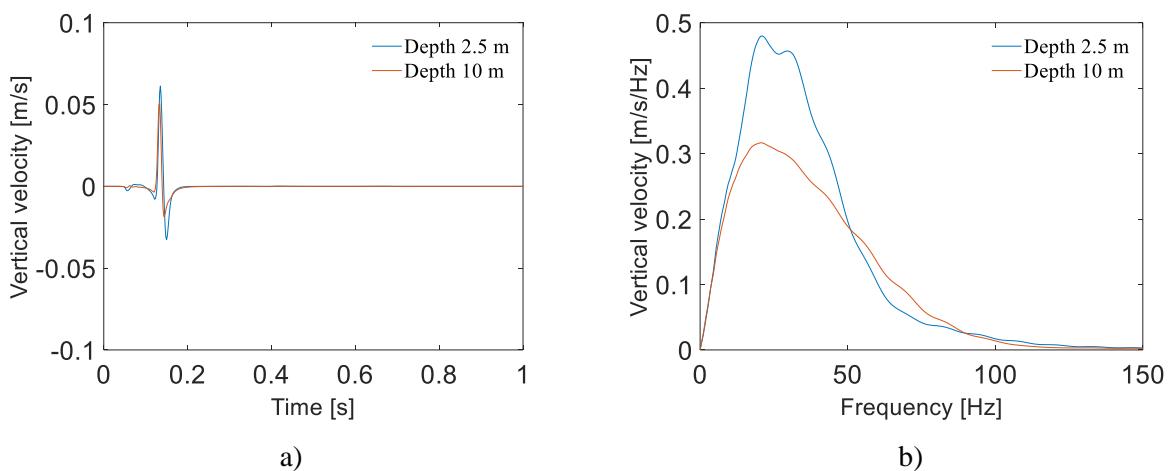


Figure 7 – Vertical particle velocity record for an observation point located at the ground surface and 15 m away from the pile center, considering pile penetration depths of 2.5 m and 10 m: a) time domain; b) frequency domain.

3.3 Vibro-acoustic building response

Taking into account the purpose of the paper, the vibro-acoustic response of the building due to the pile driving operations is analysed. Thus, a finite element structural model was developed using the commercial software Ansys [25], as depicted in Figure 8a). The choice of this software is due to the possibility of extracting mass and stiffness matrices, allowing the use of some routines developed in MatLab by the authors to perform dynamic analysis.

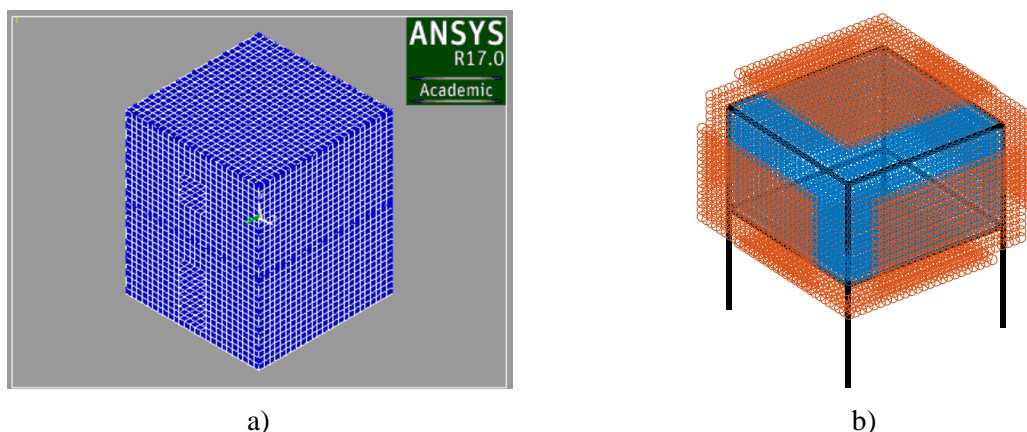


Figure 8 – Vibro-acoustic analysis: a) finite element model developed in the software Ansys; b) schematic representation of the collocation points and virtual sources used in the MFS numerical model (blue dots – collocation points along the boundaries; red dots – virtual sources outside the acoustic domain).

Since particle vibration velocity is usually correlated with structural damage, it is fundamentally important to predict the vibration levels in terms of vibration particle velocities. Figure 9 shows the time history and frequency content of particle velocity for two points located in the centre of the slab of the 1st floor, considering pile penetration depths of 2.5 m and 10 m.

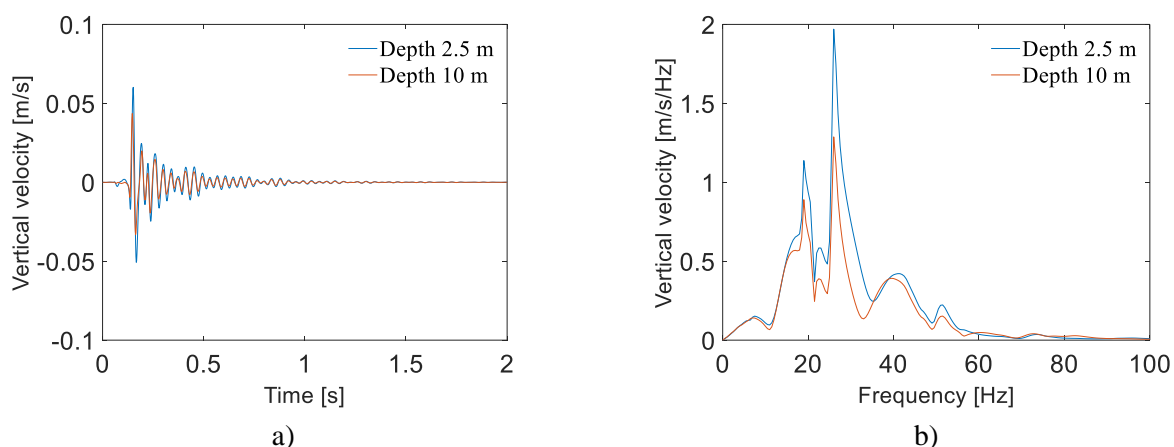


Figure 9 – Vertical particle velocity record for pile penetration depths of 2.5 m (blue line) and 10 m (red line) and the observation point located in the center of the 1st floor slab: a) time domain; b) frequency domain.

The trend verified in the ground response in terms of penetration depths and vibration levels is, as expected, confirmed in the building response: lower penetration depths of the pile give rise to larger maximum vibration levels. On the other hand, similar peak vibration levels are observed between the

building and the free-field responses. This aspect is highly influenced by the dynamic behaviour of the building, especially in what concerns to the natural frequencies of the slabs and to the frequency content of the excitation.

Despite the similarity of vibration peak values between the response at the free-field and in the structure, in what concerns the frequency content the differences are quite evident. In fact, the dynamic behaviour of the structure is fundamental in the results evaluated, as previously highlighted.

Moving to the acoustic analysis, it is object of study the quantification of the sound pressure levels in the centre of the interior space corresponding to the 1st floor of the building induced by the vibration of its own structural elements. The application of the 3D MFS model requires the definition of a set of collocation points and virtual sources, schematically represented in Figure 8b). Thus, the time history and frequency content of the sound pressure for an observation point located in the centre of the acoustic space and for pile penetration depths of 2.5 m and 10 m are depicted Figure 10.

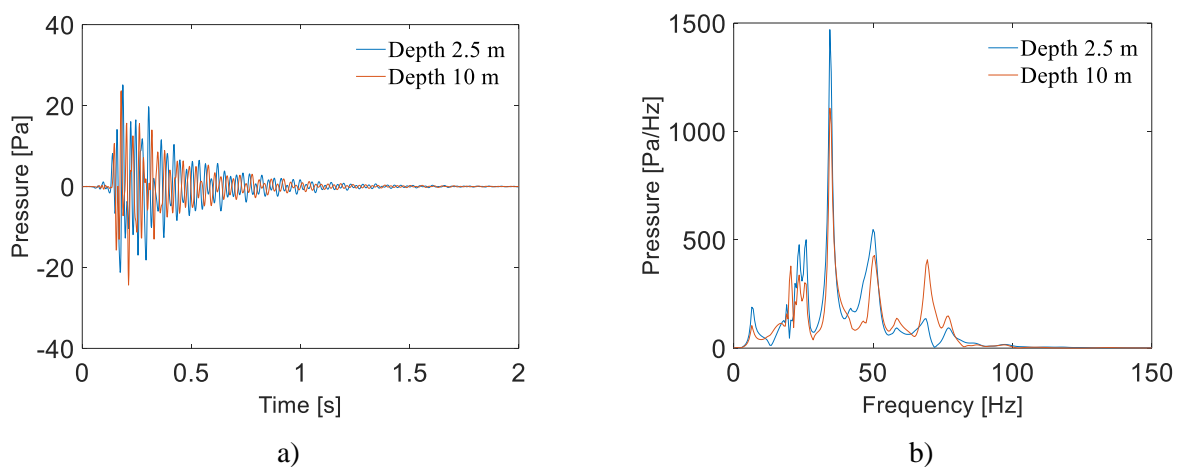


Figure 10 – Acoustic response for a point on the center of the interior space of the 1st floor, considering pile penetration depths of 2.5 m (blue line) and 10 m (red line): a) time domain; b) frequency domain.

As can be seen from the results in Figure 10, there is a similar acoustic response trend for the two pile penetration depths analysed, although with slight lower values for the higher depths. Comparatively with the elastodynamic response of the building, it should be highlighted the wide frequency content of the first, with significant content until almost 100 Hz. This aspect has significance in the acoustic response of the building, contributing to the excitation of higher-order acoustic modes.

4 Conclusions

A generalist and efficient modelling approach to address vibro-acoustic problems induced by pile driving, contemplating the simulation of the hammer-pile-ground-building system was presented. Based on a sub-structuring methodology, the pile-ground domain is model by a FEM-PML approach in axisymmetric conditions and the impact force evaluated using a two degrees of freedom model (simulation of the hammer device). The building simulation is performed by a 3D FEM approach, adequately adapted to take into account the soil-structure interaction, where the dynamic stiffness of the ground is evaluated through a lumped-parameter model. The acoustic field induced by the structural vibration is analysed by a 3D MFS model, which allows describing the response of the acoustic medium in an efficient way.

After the model description, a brief case study was presented, where the ground-building response was analysed for two pile penetration depths, allowing identify the reduced influence of this parameter for this specific case. In fact, just a slight reduction of the maximum vibration velocities was found with the increase of the pile penetration depth. However, the aspect to highlight in this work is the suitability of the proposed methodology for dealing with this type of phenomenon, being a versatile prediction tool for the assessment of ground-borne noise and vibration induced by pile driving.

Acknowledgements

This work was financially supported by: Programmatic funding - UIDP/04708/2020 of the CONSTRUCT - Instituto de I&D em Estruturas e Construções - funded by national funds through the FCT/MCTES (PIDDAC); Project POCI-01-0145-FEDER-029577 and Project POCI-01-0145-FEDER-029634 – both funded by FEDER funds through COMPETE2020 – Programa Operacional Competitividade e Internacionalização (POCI) and by national funds (PIDDAC) through FCT/MCTES.



References

- [1] Hindmarsh, J.J. and W.L. Smith, *Quantifying construction vibration effects on daily radiotherapy treatments*. Journal of Applied Clinical Medical Physics, 2018. **19**(5): p. 733-738.
- [2] Rahman, N.A.A., A.A. Musir, N.H. Dahalan, A.N.A. Ghani, and M.K.A. Khalil. *Review of vibration effect during piling installation to adjacent structure*. 2017.
- [3] Cleary, J.C. and E.J. Steward, *Analysis of ground vibrations induced by pile driving and a comparison of vibration prediction methods*. DFI Journal - The Journal of the Deep Foundations Institute, 2016. **10**(3): p. 125-134.
- [4] Massarsch, K.R. and B.H. Fellenius, *Ground vibrations induced by impact pile driving*, in *6th International Conference on Case Histories in Geotechnical Engineering*. 2008: Arlington. p. 1-38.
- [5] Ramshaw, C.L., A.R. Selby, and A.R. Bettles, *Computation of ground waves due to piling*, in *Application of Stress Wave Theory to Piles* 2000. p. 495-502.
- [6] Khoubani, A. and M.M. Ahmadi, *Numerical study of ground vibration due to impact pile driving*. Proceedings of the Institution of Civil Engineers: Geotechnical Engineering, 2014. **167**(1): p. 28-39.
- [7] Hodayoun Rooz, A.F. and A. Hamidi, *A numerical model for continuous impact pile driving using ALE adaptive mesh method*. Soil Dynamics and Earthquake Engineering, 2019. **118**: p. 134-143.
- [8] Masoumi, H.R., G. Degrande, and G. Lombaert, *Prediction of free field vibrations due to pile driving using a dynamic soil-structure interaction formulation*. Soil Dynamics and Earthquake Engineering, 2007. **27**(2): p. 126-143.
- [9] Masoumi, H.R., G. Degrande, and A. Holeyman, *Pile response and free field vibrations due to low strain dynamic loading*. Soil Dynamics and Earthquake Engineering, 2009. **29**(5): p. 834-844.
- [10] Mont'Alverne Parente, C., P.A. Costa, and A.S. Cardoso. *Ground-borne vibrations induced by pile driving: Prediction based on numerical approach*. in *Advances in Engineering Materials, Structures and Systems: Innovations, Mechanics and Applications - Proceedings of the 7th International Conference on Structural Engineering, Mechanics and Computation*, 2019. 2019.

- [11] Quagliata, A., M. Ahearn, E. Boeker, C. Roof, L. Meister, and H. Singleton, *Transit Noise and Vibration Impact Assessment Manual*. 2018, Federal Transit Administration - Department of Transportation, Office of Planning and Environment. Washington DC.
- [12] Aubry, D. and D. Clouteau, *A subdomain approach to dynamic soil-structure interaction*, in *Recent Advances in Earthquake Engineering and Structural Dynamics*, D.V.a.C. RW, Editor. 1992, Ouest Editions/AFPS: Nantes. p. 251-272.
- [13] Pyl, L., G. Degrande, and D. Clouteau, *Validation of a source-receiver model for road traffic induced vibrations in buildings. II: Receiver model* Journal of Engineering Mechanics, 2004. **130**(12): p. 1394-1406.
- [14] Lopes, P., P. Alves Costa, M. Ferraz, R. Calçada, and A. Silva Cardoso, *Numerical modelling of vibrations induced by railway traffic in tunnels: from the source to the nearby buildings*. Soil Dynamics and Earthquake Engineering, 2014. **61-62**: p. 269-285.
- [15] Lopes, P., P. Alves Costa, R. Calçada, and A. Silva Cardoso, *Influence of soil stiffness on vibrations inside buildings due to railway traffic: numerical study*. Computers & Geotechnics, 2014. **61**: p. 277-291.
- [16] Fiala, P., G. Degrande, and F. Augusztinovicz, *Numerical modelling of ground-borne noise and vibration in buildings due to surface rail traffic*. Journal of Sound and Vibration, 2007. **301**(3-5): p. 718-738.
- [17] François, S., L. Pyl, H. Masoumi, and G. Degrande, *The influence of dynamic soil-structure interaction on traffic induced vibrations in buildings*. Soil Dynamics and Earthquake Engineering, 2007. **27**(7): p. 655-674.
- [18] Nagy, A.B., P. Fiala, F. Márki, F. Augusztinovicz, G. Degrande, S. Jacobs, and D. Brassensx, *Prediction of interior noise in buildings generated by underground rail traffic*. Journal of Sound and Vibration, 2006. **293**(3-5): p. 680-690.
- [19] Løvholt, F., K. Norèn-Cosgriff, C. Madshus, and S.E. Ellingsen, *Simulating low frequency sound transmission through walls and windows by a two-way coupled fluid structure interaction model*. Journal of Sound and Vibration, 2017. **396**: p. 203-216.
- [20] Neves E Sousa, A. and B.M. Gibbs, *Low frequency impact sound transmission in dwellings through homogeneous concrete floors and floating floors*. Applied Acoustics, 2011. **72**(4): p. 177-189.
- [21] Park, H.S., B.K. Oh, Y. Kim, and T. Cho, *Low-frequency impact sound transmission of floating floor: Case study of mortar bed on concrete slab with continuous interlayer*. Building and Environment, 2015. **94**: p. 793-801.
- [22] Colaço, A., P. Alves Costa, P. Amado-Mendes, F. Magalhães, and L. Godinho, *Experimental validation of a FEM-MFS hybrid numerical approach for vibro-acoustic prediction*. Applied Acoustics, 2018. **141**: p. 79-92.
- [23] Masoumi, H. and G. Degrande, *Numerical modeling of free field vibrations due to pile driving using a dynamic soil-structure interaction formulation*. Journal of Computational and Applied Mathematics, 2008. **215**(2): p. 503-511.
- [24] Furtado, A., H. Rodrigues, A. Arêde, and H. Varum, *Mechanical properties characterization of different types of masonry infill walls*. Frontiers of Structural and Civil Engineering, 2020. **14**(2): p. 411-434.
- [25] ANSYS® *Academic Research Mechanical, Release 17.0, Help System, Coupled Field Analysis Guide*, ANSYS, Inc.